P3.3   A numerical investigation of supercells in landfalling tropical cyclones

Matthew J. Morin*
Matthew D. Parker
Kevin A. Hill
Gary M. Lackmann
Department of Marine, Earth, & Atmospheric Sciences
North Carolina State University, Raleigh, North Carolina

1.   INTRODUCTION

Landfalling tropical cyclones (TCs) often produce supercells reminiscent of their Great Plains counterparts. TC supercells themselves are often referred to as "miniature supercells" (e.g., McCaul 1991), with a typical mesocyclone diameter and depth of 5-7 and 4 km, respectively (Eastin and Link 2009), which makes them harder to detect on radar compared to the typical Great Plains supercell. These supercells can spawn tornadoes capable of considerable damage, posing a serious threat to the Gulf and Atlantic coasts for hundreds of kilometers inland, south and west of Virginia (Schultz and Cecil 2009). In fact, McCaul (1991) showed that approximately 59% of landfalling TCs in a 39-year data set produced at least one reported tornado.

This study aims to understand the environmental and physical mechanisms that lead up to tornadogenesis in a TC supercell. Our knowledge of TC supercells is not as comprehensive as their continental counterparts due in part to the observation limitations of these storms when they are offshore and due to their comparatively smaller sizes and lifetimes. Tornadic TC supercells are most prolific in the TC's right-front quadrant (RFQ; with respect to TC forward motion) and these cells are usually embedded in the TC's rainbands. Some observational studies mention a possible correlation between TC tornadogenesis and a collocation of a midlevel dry air intrusion and/or low-level boundary (e.g., McCaul 1987; Baker et al. 2009). Some authors (e.g., Baker et al. 2009) have also speculated that landfall induces favorable changes in the low-level hodographs inside TCs. Further, some observational studies have noted a diurnal signal in the number of TC tornadoes during outbreaks (e.g., Curtis 2004; Schultz and Cecil 2009). However, questions still remain as to what differentiates the environments of small, short-lived, TC supercells versus those that are larger and longer-lived.

To address the aforementioned gaps in the knowledge base, our study uses idealized numerical simulations to run a series of sensitivity tests where TC supercells evolve in different environments.

Our working hypotheses are as follows.

- The sea-to-land transition is a crucial factor in TC supercell intensification due to the impacts of a larger diurnal temperature variation and increased surface friction over land.

- The storm-scale processes that lead to updraft rotation are enhanced in supercells that develop in and near dry air intrusions due to (1) localized midlevel evaporational cooling in the typically moist TC environment, and (2) cloud erosion, which leads to increased surface insolation during the day.

As part of our ongoing research, the net effects of these processes are investigated in both maritime and landfalling TCs.

2.   DATA AND METHODS

Our hypotheses are tested using the Advanced Research WRF (WRF-ARW) model version 2.2.1 (Skamarock et al. 2005) to scrutinize supercells embedded within the rainbands of an idealized TC. The motivation for using an idealized model framework is that, used in conjunction with a series of sensitivity tests, we can isolate the specific role that an environmental ingredient has on our simulated supercells.

Rather than simply running a storm-scale model where convective cells are artificially triggered in a horizontally homogeneous environment, this study is novel in that we have created a setting where supercells form naturally in the rainbands of a credible TC. To accomplish this, we use a triply-nested domain setup (Fig. 1). The outermost domain, with a grid spacing of 18 km, is remarkably large for the purpose of allowing a wide buffer zone between the

*Corresponding author address: Matthew J. Morin, Department of Marine, Earth, & Atmospheric Sciences, North Carolina State University, Campus Box 8208, Raleigh, NC 27695–8208. E-mail: mjmorin@ncsu.edu

westward-moving TC and the domain's boundaries. The first two nests, with grid spacings of 6 and 2, respectively, are vortex-tracking. The fourth (and finest) model domain is the primary source of data for this study and is launched during certain 10-hour periods during the full 10-day simulation. Domain 4 has a grid spacing of 667 m, is stationary, and covers a radial distance of approximately 775 km in the TC's RFQ, since this is where climatology shows a high occurrence of tornadic TC supercells (e.g., Schultz and Cecil 2009).

Given the compound nature of our hypotheses, we configured multiple sensitivity tests where individual aspects can be isolated. In this study there is one reference experiment (i.e., the "control" run) that features a TC over the open ocean, and simulations where the TC is in the presence of a simulated midlevel dry air intrusion, allowed to make landfall (at different times of the day), or both. A description of each type of simulation is presented in the next subsections.

2.1 Initial conditions

A hurricane is spawned by placing a bogus vortex in an otherwise horizontally homogeneous initial environment. The Jordan (1958) average "hurricane season" temperature profile and an idealized moisture profile are used to initialize the model. Our idealized moisture profile does not feature the subsidence drying that is typical in the Caribbean, where the Jordan (1958) "hurricane season" soundings were taken. Our ambient wind profile is based on Hurricane Ivan (2004) from Fig. 9/Table 1 of Baker et al. (2009). Our moderately-sheared wind profile results in a TC steering speed of around 5.5 m s^{-1}, which matches the climatological value associated with peak reports of TC tornadoes (e.g., Schultz and Cecil 2009). We configured a 20° f-plane to accommodate a straight-moving TC throughout the 10-day simulation. Since our aim is to study supercells in a "middle of the road" quasi-steady category 3 TC, a sea surface temperature of 26°C was used. Since we have not coupled an ocean model to WRF, SSTs remain the same throughout the simulations and are not affected by cold upwelling beneath the TC. We view this as acceptable, because our research goals are to study the embedded supercells within a category 3 storm, not to study the processes governing TC intensity itself.

2.2 Idealized landfall

For the landfall simulations, our TC makes landfall as a quasi-steady category 3 hurricane. Because this is a TC-supercell study, "landfall", for our purposes, is defined as around the time when isolated cells within the outer rainband first pass over the coastline. The land surface in our model is highly idealized and its properties (e.g., albedo, friction, vegetation) represent typical values found in North Carolina. The terrain is flat and its characteristics are horizontally homogeneous. TC landfall is also idealized, with the heading being perpendicular to the coastline. This study includes simulations where landfall occurs at local noon and alternatively at local midnight. High-resolution storm-scale analysis is performed on cells in the RFQ from a few hours before making landfall through two days after landfall. TC-tornado climatology shows that the number of TC-tornado occurrences significantly drops off 48 hours after the TC makes landfall (e.g., Schultz and Cecil 2009).

2.3 Midlevel dry air intrusion

Another novel aspect of this study is the inclusion of a simulated midlevel dry air intrusion. In these simulations, a "pool" of comparatively drier air is introduced gradually in a specified location within the mid troposphere ahead of the TC. The location for the area of artificial drying is observationally-based and allows the TC to eventually entrain some of the dry air into its circulation in a similar manner to the "type 2" source in Curtis (2004). Our simulated midlevel dry air intrusion is well-established in the RFQ as the outer rainband supercells start making landfall. The resultant RFQ relative humidity profile within the dry air intrusion has remarkable similarities to those sampled in real observed cases (e.g., Curtis 2004; Baker et al. 2009). Detailed analysis of how this dry air intrusion influences the embedded supercells is ongoing.

2.4 Mesocyclone detection algorithm

This study uses a set of updraft-helicity-based metrics that enable us to compare the population of simulated supercells among the various simulations, allowing us to generate suitable statistics for testing our hypotheses. Helical updrafts are identified by computing updraft helicity (Kain et al. 2008), which quantifies the degree to which strong updrafts and positive vertical vorticity are correlated. Thus we are able to create a map of the location of every supercell in the domain as well as compute statistics on the ensemble of supercells, rather than just analyzing one "best case" cell. Our algorithm detects and tracks 1-4 km updraft helicity exceeding 550 m^2 s^{-2} (with a minimum area of approximately

3.5 km^2). Our choices of an updraft helicity threshold and minimum area represent values that were subjectively determined to maximize probability of detection for mesocyclones while keeping the false alarm rate as low as possible for what we concluded were spurious circulations.

3. OVERVIEW OF QUASI-IDEALIZED TC

The minimum sea level pressure (SLP) in the control run for the first eight days is shown in Figure 2. The innermost domain is launched for high-resolution storm-scale analysis after day 5, which is around the time cells in the outer rainband would start making landfall in the landfall simulations. A snapshot of the portion of the TC resolved in this, our 667 m grid, is provided in Figure 3. The idealized model framework produces a credible TC with a pronounced rainband. Additional figures featuring our landfall and dry air intrusion simulations will be presented at the conference.

4. HIGH-RESOLUTION TC SUPERCELL ANALYSIS

Detailed analysis of our simulated supercells is in progress. Preliminary results show well-resolved supercells embedded within the TC's inner and outer rainbands on our 667 m grid. Besides their appearance in simulated radar reflectivity images, TC supercells are also confirmed by the presence of a helical updraft (Fig. 4). Supercells in our highest-resolution domain bear remarkable resemblance to those observed on radar during real landfalling TC events (e.g., Baker et al. Fig. 6c-e). Other encouraging findings indicating supercells include weak echo vaults and velocity enhancement signatures (Schneider and Sharp 2007) in the simulated radar reflectivity and radial velocity data, which will be discussed in further detail at the conference. Also of great interest is the observation of strong, long-lived supercells as identified by our mesocyclone tracking algorithm (e.g., red tracks in Figure 5). Calculation of statistics for the population of mesocylones in each run is currently ongoing.

5. FUTURE WORK

A plethora of model output has been generated, from five full 10-day TC simulations, each containing four separate 10-hour high-resolution analysis windows. An overview of these simulations, as well as some of our preliminary findings, will be presented at the conference. One of our long-term goals is to offer a clearer explanation of the key processes that take place during TC supercell intensification. By comparing the numbers, strengths, and lifetimes of mesocyclones from run to run and time window to time window, we hope to provide operationally useful information about the key environmental ingredients for TC supercells and tornadoes. It is not hard to imagine additional model configurations that could also be attempted (different storm motion vectors, coastal angles, TC intensities, etc.).

In addition to the aforementioned full-TC simulations, this study will utilize "benchmark" simulations using a horizontally homogeneous initial condition. This series of simulations will provide storm-scale analysis of a supercell initiated by a warm bubble (as well as by convergence forcing) in a single sounding "TC supercell" environment, which is taken from the finest grid of the full-TC simulations. The purpose of these simplified benchmark runs, generally speaking, is to determine whether or not the hurricane itself needs to be simulated in order to produce realistic TC supercells.

References

Baker, A. K., M. D. Parker, and M. D. Eastin, 2009: Environmental ingredients for supercells and tornadoes within Hurricane Ivan. *Wea. Forecasting*, **24**, 223–244.

Curtis, L., 2004: Midlevel dry intrusions as a factor in tornado outbreaks associated with landfalling tropical cyclones from the atlantic and gulf of mexico. *Wea. Forecasting*, **19**, 411–427.

Eastin, M. D. and M. C. Link, 2009: Miniature supercells in an offshore outer rainband of Hurricane Ivan (2004). *Mon. Wea. Rev.*, **137**, 2081–2104.

Jordan, C. L., 1958: Mean soundings for the West Indies area. *J. Meteor.*, **15**, 91–97.

Kain, J. S., S. J. Weiss, D. R. Bright, M. E. Baldwin, J. J. Levit, G. W. Carbin, C. S. Schwartz, M. L. Weisman, K. K. Droegemeier, D. B. Weber, and K. W. Thomas, 2008: Some practical considerations regarding horizontal resolution in the

first generation of operational convection-allowing NWP. *Wea. Forecasting*, **23**, 931–952.

McCaul, E. W., Jr., 1987: Observations of the Hurricane "Danny" tornado outbreak of 16 August 1985. *Mon. Wea. Rev.*, **115**, 1206–1223.

———, 1991: Buoyancy and shear characteristics of hurricane-tornado environments. *Mon. Wea. Rev.*, **119**, 1954–1978.

Schneider, D. and S. Sharp, 2007: Radar signatures of tropical cyclone tornadoes in central North Carolina. *Wea. Forecasting*, **22**, 278–286.

Schultz, L. A. and D. J. Cecil, 2009: Tropical Cyclone Tornadoes, 1950-2007. *Mon. Wea. Rev.*, **137**, 3471–3484.

Skamarock, W. C., J. B. Klemp, J. Dudhia, D. O. Gill, D. M. Barker, W. Wang, and J. G. Powers, 2005: A description of the Advanced Research WRF Version 2. Tech. Rep. NCAR/TN-468+STR.
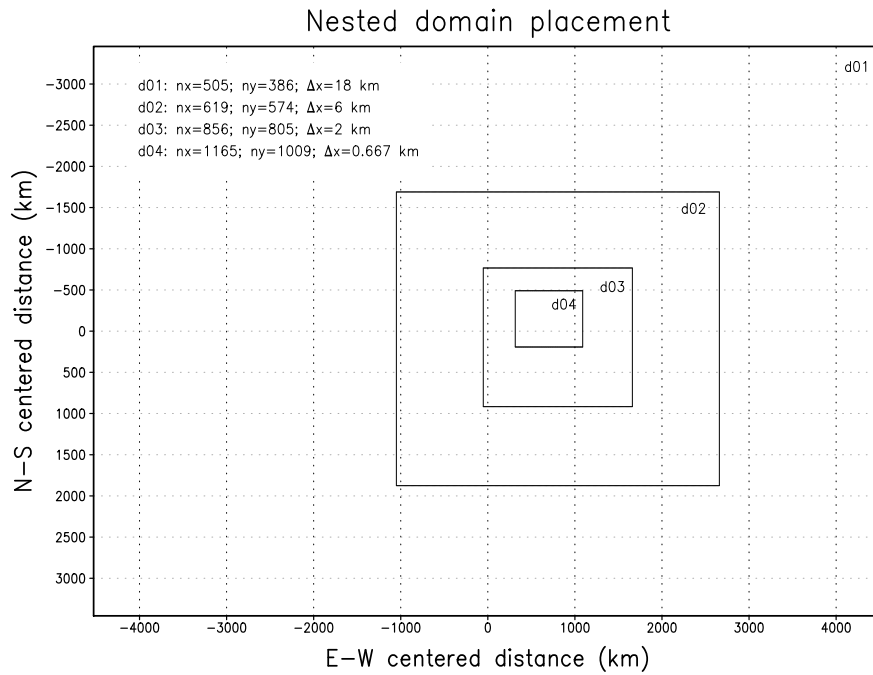
Nested domain placement

d01: nx=505; ny=386; Δx=18 km
d02: nx=619; ny=574; Δx=6 km
d03: nx=856; ny=805; Δx=2 km
d04: nx=1165; ny=1009; Δx=0.667 km

Figure 1: Schematic of the idealized TC simulation model domains.
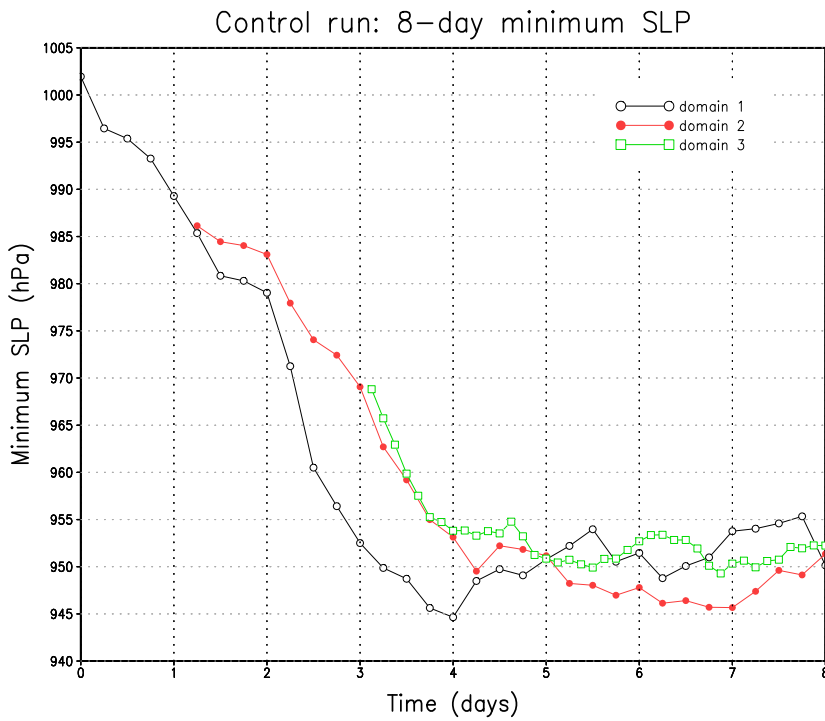
Control run: 8−day minimum SLP

Figure 2: Minimum SLP (hPa) for the control run for domains 1 (black), 2 (red), and 3 (green).

Control run: 1600 LST on day 5

Simulated visible satellite imagery

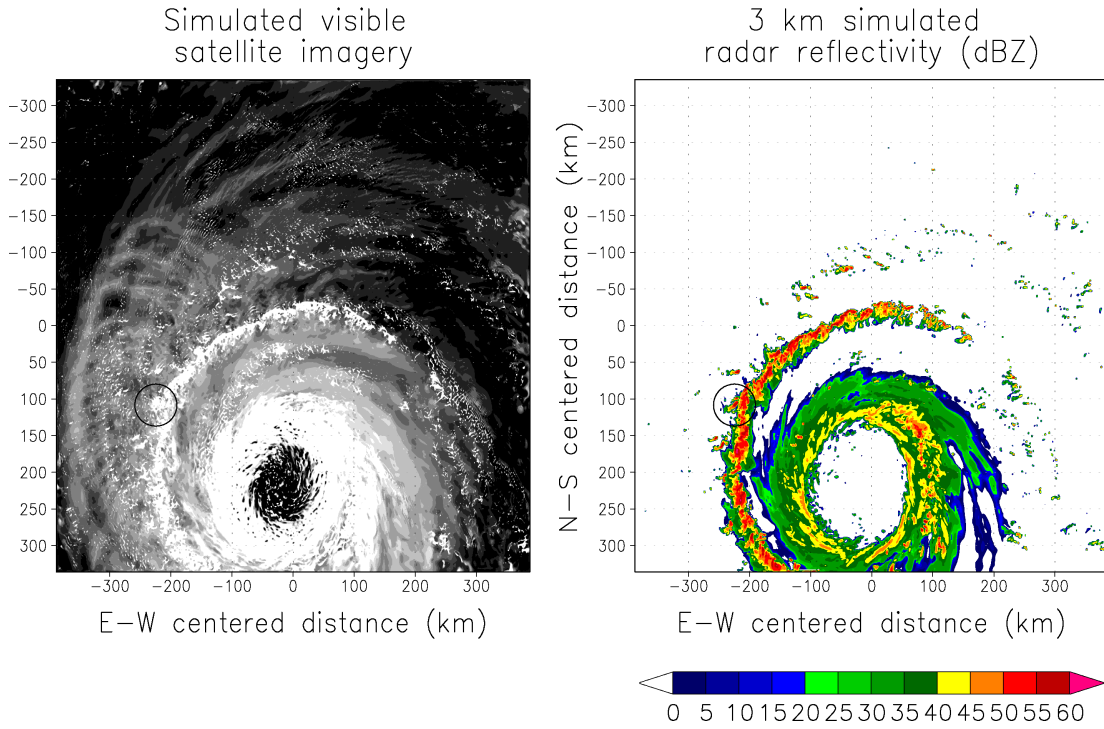### 3 km simulated radar reflectivity (dBZ)

Figure 3: Simulated visible satellite imagery (left) and 3 km radar reflectivity (right) for the control run on the 667 m grid. The black circle in each panel indicates the location of the supercell shown in Figure 4.

Control run: 1.5 km wind vectors and simulated radar reflecitivty
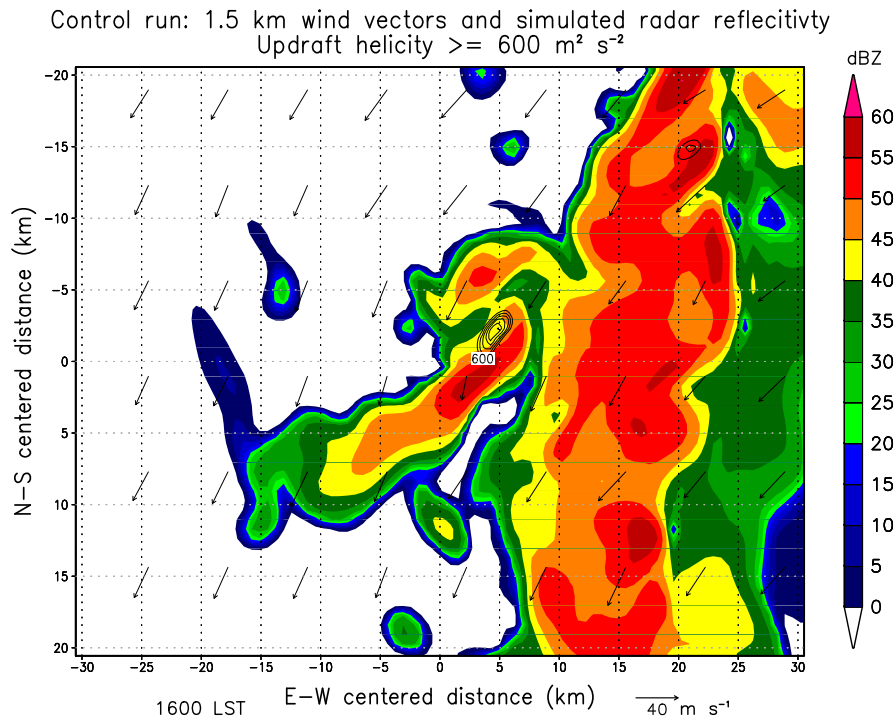### Updraft helicity >= 600 m² s⁻²

1600 LST

Figure 4: Outer rainband supercell noted in Figure 3. Simulated 1.5 km radar reflectivity (dBZ) is shaded and updraft helicity greater than or equal to 600 m² s⁻² is contoured. 1.5 km wind vectors are provided to show the general movement of cells in this area.

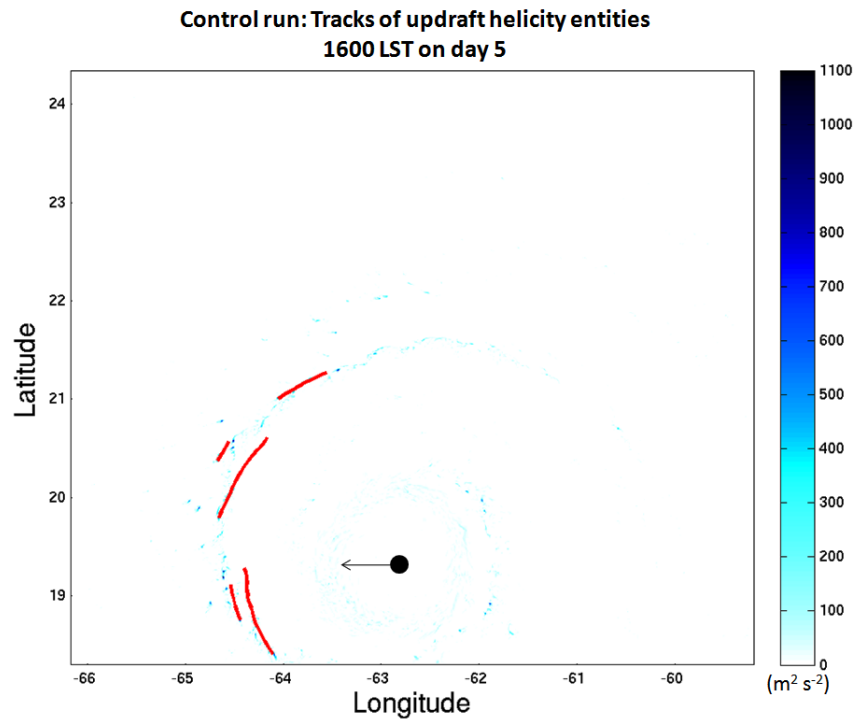**Control run: Tracks of updraft helicity entities**
1600 LST on day 5

Figure 5: Tracks of cells that surpass the updraft helicity threshold and minimum area restriction in the control run. The black dot represents the estimated location of the TC eye, while the arrow denotes the direction of TC motion. Recalling that the simulations are run on an f-plane, latitude values here are somewhat arbitrary, but are defined as such for the purposes of our blob tracking algorithm. Figure 3 provides a clearer picture of the location and structure of the rainband responsible for generating these particular rotating storms.